PHOTONICS Research

Towards simultaneous observation of path and interference of a single photon in a modified Mach–Zehnder interferometer

FENGHUA QI,[1,†] ZHIYUAN WANG,[1,†] WEIWANG XU,[1] XUE-WEN CHEN,[1,4] AND ZHI-YUAN LI[2,3]

[1]School of Physics and Wuhan National Laboratory for Optoelectronics, Huazhong University of Science and Technology, Wuhan 430074, China
[2]College of Physics and Optoelectronics, South China University of Technology, Guangzhou 510641, China
[3]e-mail: phzyli@scut.edu.cn
[4]e-mail: xuewen_chen@hust.edu.cn

Received 27 December 2019; revised 10 February 2020; accepted 11 February 2020; posted 13 February 2020 (Doc. ID 386774); published 1 April 2020

Classical wisdom of wave–particle duality regulates that a quantum object shows either the particle or wave nature but never both. Consequently, it would be impossible to observe simultaneously the complete wave and particle nature of the quantum object. Mathematically the principle requests that the interference visibility V and which-path distinguishability D satisfy an orthodox limit of $V^2 + D^2 \leq 1$. The present work reports a new wave–particle duality test experiment using single photons in a modified Mach–Zehnder interferometer to demonstrate the possibility of breaking the limit. The key element of the interferometer is a weakly scattering total internal reflection prism surface, which exhibits a pronounced single-photon interference with a visibility of up to 0.97 and simultaneously provides a path distinguishability of 0.83. Apparently, the result of $V^2 + D^2 \approx 1.63$ exceeds the orthodox limit set by the classical principle of wave–particle duality for single photons. We expect that more delicate experiments in the future should be able to demonstrate the ultimate limit of $V^2 + D^2 \approx 2$ and shed new light on the foundations of contemporary quantum mechanics.

https://doi.org/10.1364/PRJ.386774

1. INTRODUCTION

The wave–particle duality of a quantum object, including photons, electrons, atoms, etc., constitutes one of the conceptual cornerstones of quantum physics. The principle dictates that all quantum objects exhibit mutually exclusive behaviors of two intrinsic attributes, namely, being either as wave or as particle depending on how they are measured, but never both [1–10]. Over the past several decades, numerous studies using *gedanken* or practical interferometers such as a Mach–Zehnder interferometer (MZI) and Young's two-slit interferometer in various genuine arrangements have been carried out to test the wave–particle duality principle of particles. To name a few, there are, for instance, Wheeler's delayed-choice scheme [6,7,11–16], Scully's quantum eraser scheme [8–10], Afshar's scheme [17–19], and others [20–23]. The outcomes of all previous test experiments can be summarized into three situations characterized by the interference visibility V and which-path distinguishability D. In the first situation, one uses a specific setup to achieve perfect observation of the wave nature of the particle with an interference visibility $V = 1$ at the price of complete loss of the path distinguishability with $D = 0$. In the second situation, one applies another setup to distinguish unambiguously the paths that each particle passes at the cost of complete destruction of the interference pattern, i.e., $V = 0$ and $D = 1$. In the third situation, using interferometer setups with quantum delayed-choice schemes, one can observe the simultaneous partial wave and partial particle nature of photons with $V \neq 0$ and $D \neq 0$ [13,15,16,23], which yet still satisfies the orthodox limit of $V^2 + D^2 \leq 1$ [24]. In summary, despite enormous efforts, all existing test experiments have shown no sign of going beyond the principle of wave–particle duality.

A rigorous analysis based on full quantum mechanics in the Schrödinger picture reveals that in previous interferometers, such as the delayed-choice scheme of MZI as well as Afshar's scheme, the measurement of one entity (either wave or particle nature) strongly disturbs the other so that the observation of the two are exclusive [25,26]. As illustrated in Fig. 1(a), a photon sent into the MZI goes either into path X or path Y with each 50% probability after the first beam splitter BS1. To know which path the photon passes and thus the particle property, one needs to remove the second beam splitter BS2 and check the detectors X and Y. To observe the interference pattern and thus the wave property of the photon, one should keep BS2 and examine the detectors X and Y. However, no matter how smart the design is, it is impossible to observe the wave and particle

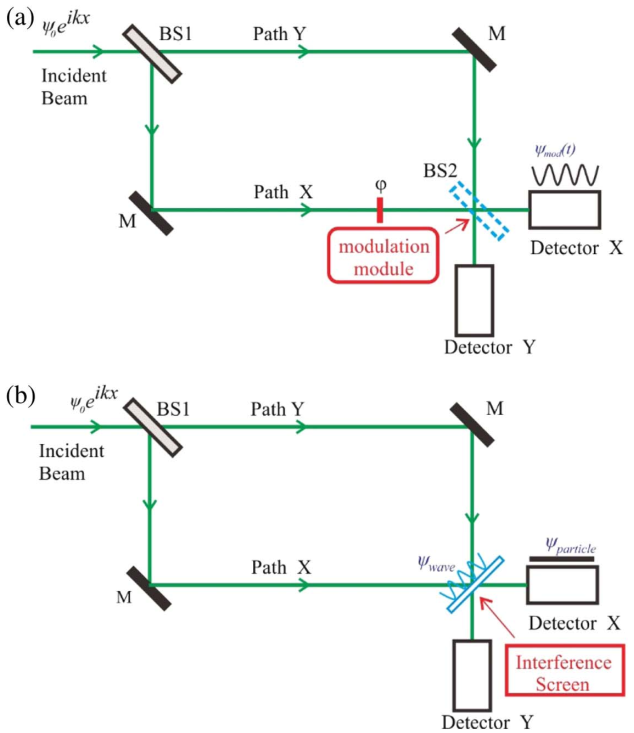

Fig. 1. (a) Schematic setup of classical Mach–Zehnder interferometer (MZI) used to test wave–particle duality of a photon. The MZI consists of the first beam splitter BS1, two mirrors (M), a phase shift (φ), and the second beam splitter BS2. BS2 can either be present in the path, or absent, or controlled by an external (classical or quantum) module. (b) Schematic setup of weak-measurement MZI (WM-MZI), where an interference screen (denoted by the blue thick lines) with high transmission and weak scattering replaces BS2.

nature of the photon simultaneously because the insertion and removal of BS2 are completely exclusive operations. Yet, as displayed in Fig. 1(b), a modified MZI working in the weak-measurement regime, hereafter called WM-MZI, can largely get around the difficult mutual exclusion problem by using an interference screen to replace BS2 in the standard MZI [27]. This interference screen exhibits a high transmission and weak scattering of the photon, and essentially becomes a detector of interference pattern via weak scattering. A similar idea has recently been extended to atom interferometers with weak-measurement path detectors [28]. Quantum mechanical analyses show that compared to the standard MZI the proposed WM-MZI has the potential to make simultaneous observation of interference and which-path information of quantum objects. Specifically, it can reach the level of $V = 1$ and $D \to 1$, so that $V^2 + D^2 \to 2$, which far exceeds the regime allowed by the principle of wave–particle duality. In this work, we experimentally construct a WM-MZI setup and perform single-photon experiment with this new interferometer to test the wave–particle duality of photons.

2. RESULTS

Simultaneous observation of the path and interference of a single photon in the WM-MZI is an intriguing while practically challenging experiment. The difficulty lies in observing the interference pattern via the WM-MZI. The proposed original configuration shown in Fig. 1(b) suffers from very low collection efficiency of weakly scattered single photons from the interference screen. For a two-dimensional image with 100×100 pixels, the average photon detection rate at each pixel is estimated to be fewer than 0.01 count per second (cps) considering a single-photon source with an emission rate of 100 kcps, a scattering efficiency of 10%, and an overall detection efficiency of 1% for the proposed configuration. To circumvent such a formidable experimental difficulty, we take advantage of the fact that the interference pattern of two plane waves is one dimensional in nature and thus one can use an efficient point detector (an avalanche photodiode, APD) with a movable slit instead of a camera to observe the interference pattern. Moreover, we modify the original high-transmission weak-scattering interference screen in Fig. 1(b) to a high-reflection weak-scattering prism setup so that a microscope objective with a high numerical aperture (NA) could be used to improve the collection of the weakly scattered single photons. The above modifications afford us to experimentally demonstrate single-photon WM-MZI, as discussed in the following sections.

Figure 2(a) shows the key element of the WM-MZI, i.e., a prism surface that hosts the interference and provides weak scattering via a diffusive scattering thin film. The weakly scattering film is made via casting a droplet of dilute milk. Single photons split into two beams are incident upon the prism surface at total internal reflection angles with an angle difference of $\theta \approx 1.75°$. Labeled as beam 1 and beam 2, the two beams exit the prism with the same separation angle and are detected by APD1 and APD2, respectively. These two beams interfere on the prism surface to form a one-dimensional interference pattern, which evanescently decays into the air side of the surface. With a diffusive weak-scattering thin film, incident single photons are scattered by a small probability and a fraction of that is collected and detected by APD3 to reveal the interference pattern. Moreover, with weak scattering the total reflection becomes imperfect, having a reflection coefficient R slightly smaller than unity. We have tested the WM-MZI setup by incidence of a laser beam and observed a very clear interference pattern at the prism hypotenuse surface, as illustrated by the right-most image in Fig. 2(a), which confirms that the weak-scattering prism surface functions nicely as an interference screen for light.

Figures 2(b) and 2(c) display the whole experimental setup. An efficient single-photon source based on spontaneous emission of excited single CdSe/CdS core–shell colloidal quantum dots (QDs) [29–33] is prepared in Room 1 and then by coupling to the single-mode fiber (SMF) the single photons are delivered to the WM-MZI setup in Room 2. The challenging part is to achieve large coupling of the single photons from single QDs into the SMF [31]. Aiming for that goal, we designed a sandwich sample structure as shown in the inset of Fig. 2(b), where the QDs are sandwiched between a coverslip and a PMMA thin film with a thickness of 300 nm so that a good amount of QD emission can be coupled to the SMF. The QD sample is excited by a 532 nm continuous-wave laser in an

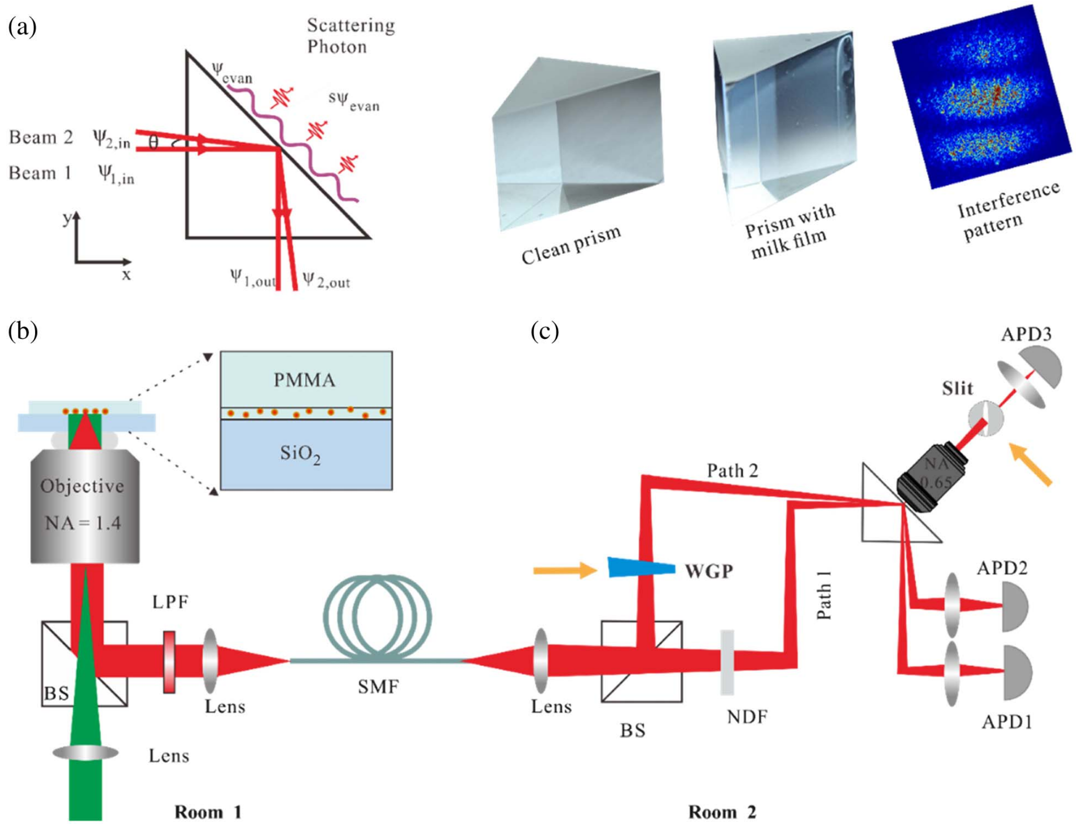

Fig. 2. Schematics of the experimental setup of the WM-MZI. (a) Single-photon interference on a prism surface coated with a weakly scattering milk film as an interference screen. The interference pattern on the right is formed by the incidence of a laser beam into the WM-MZI setup. (b) A single-mode fiber (SMF) output single-photon source apparatus. Inset shows the sample structure where CdSe/CdS coreshell quantum dots (QDs) in PMMA serve as single-photon emitters. LPF, long-pass filter. (c) WM-MZI setup. The avalanche photon detectors APD1 and APD2 record two path way information, respectively. A wedge glass plate (WGP) is used to tune the optical length of path 1. APD3 with a position-tunable slit is for observing the interference pattern.

inverted microscope configuration and the fluorescent emission around 650 nm is filtered with a long-pass filter and coupled into an SMF. We manage to have a coupling efficiency of about 15% such that the single-photon emission rate at the output of the SMF reaches about 100 kcps. As depicted in Fig. 2(c), streams of single photons from the SMF are split into two arms via a 50∶50 beam splitter and sent to the prism for the WM-MZI experiment as discussed previously. The optical path of one arm (path 2) is tunable via a wedge glass plate and a neutral density filter (0.3 OD) in the other arm is used to balance the photon count rates of the two arms. The weakly scattered photons are collected by a microscope objective with an NA of 0.65 and sent to APD3 with a slit (150 μm width) for recording the interference pattern. We note that the size of the interference pattern is about 10 mm at the position of the slit. Since a point detector APD3 is used here, the slit functions as an interference-image sampler along one direction where the interference occurs.

Before launching the wave–particle duality test experiment, we characterize the setup and properties of the single-photon light source. We first measure the reflection of the prism surface with a weakly scattering film by comparing the reflected light intensity from a silver mirror for the same source. The color-coded intensity time traces in Figs. 3(a) and 3(b) show the typical blinking phenomena of the photoluminescence (PL) from a single QD. Despite decade-long research efforts in developing nonblinking QDs [34,35], PL blinking is quite common among colloidal QDs especially when the QDs are under relatively strong excitation. QD blinking happens when the QD under constant excitation randomly switches between emission states of different brightness, possibly due to charging [33,34]. We can decipher different emission brightness states of the QD [33] and only choose the bright state to evaluate the reflectivity. With the consideration of the reflectivity of the silver mirror and two other surfaces of the prism, we estimate from the change of the average intensities of the two cases that the reflectivity of the prism coated with a weakly scattering thin film is around 83.3%. Figure 3(c) displays the second-order photon correlation function $g^{(2)}(\tau)$, where a pronounced anti-bunching dip at zero delay confirms single-photon statistics of the source [29,32]. A spectrum of the single-photon source is shown in the inset of Fig. 3(c). Since APD3 will be used to detect the interference from a very weak signal, its dark count rate is characterized and shown as a function of time in Fig. 3(d). An average dark account rate of 32 cps is measured and subtracted from the measured results obtained in the following.

It is valuable to make a quantum mechanical analysis of this WM-MZI and clarify its operation principle. The spatial

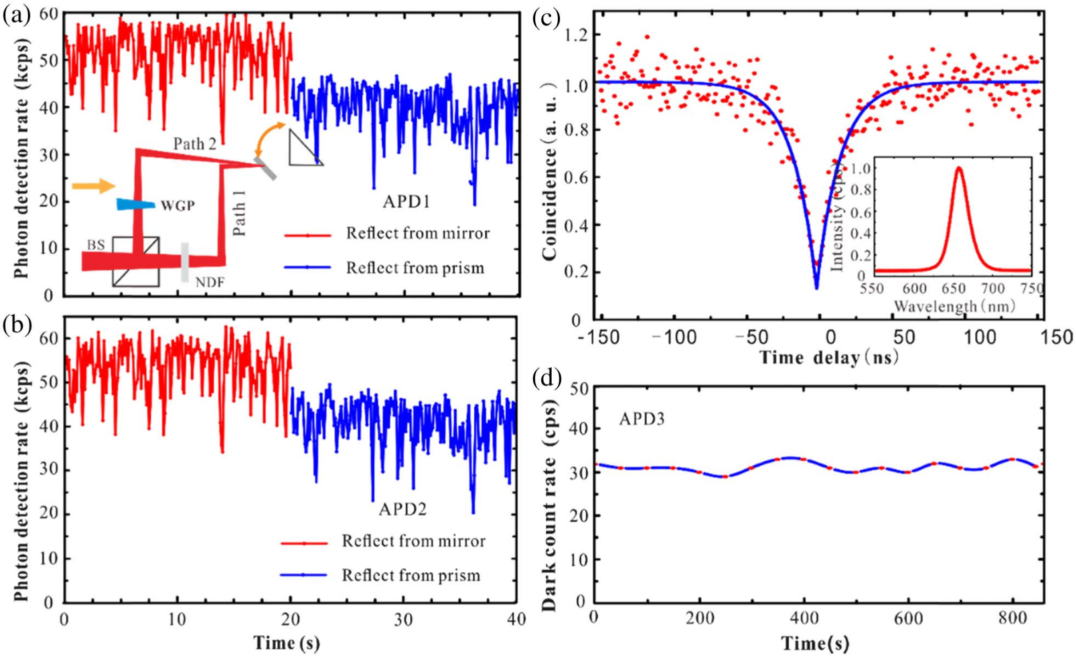

Fig. 3. Characterization of the photon paths of the setup. (a) Time traces of the photon detection rates of APD1 for the cases of reflection from a silver mirror (red) and refection from the prism surface (blue), respectively. Inset shows a schematic diagram of the measurement. (b) The same for APD2. (c) Coincidence measurement of the photon detection events of APD1 and APD2. Inset shows the spectrum of the photons in APD1 and APD2. (d) Dark count rate of APD3 as a function of time.

distributions of two incident single-photon beams can be described by two wave functions:

$$\psi_{1,\mathrm{in}}(x,y)=\psi_0 e^{ikx+i\varphi}, \tag{1a}$$

$$\psi_{2,\mathrm{in}}(x,y)=\psi_0 e^{ik(x\cos\theta-y\sin\theta)}. \tag{1b}$$

Here $k=2\pi/\lambda$ is the wavenumber of the photon with wavelength λ and φ is the phase shift of path 1 relative to path 2. The wave functions of the reflected beams read

$$\psi_{1,\mathrm{out}}(x,y)=r\psi_0 e^{-iky+i\varphi}, \tag{2a}$$

$$\psi_{2,\mathrm{out}}(x,y)=r\psi_0 e^{ik(x\sin\theta-y\cos\theta)}. \tag{2b}$$

The reflection coefficient r is close to 1. The two beams interfere on the prism hypotenuse and the total field is evanescent into the air side of the surface. Its wave function can be written as

$$\begin{aligned}\psi_{\mathrm{evan}}(x,y)&=t\psi_0\left[e^{\frac{ikn\sin(\frac{\pi}{4}+\theta_1)(x-y)}{\sqrt{2}}}+e^{\frac{ikn(x-y)}{2}+i\varphi}\right]\\&\approx 2\psi_0\left[e^{\frac{ikn(\sin\theta_1+\cos\theta_1)(x-y)}{2}}+e^{\frac{ikn(x-y)}{2}+i\varphi}\right].\end{aligned} \tag{3}$$

The scattered wave distribution recorded by APD3 can be given as

$$\begin{aligned}\psi_{\mathrm{scat}}(x,y)&=s\psi_{\mathrm{evan}}(x,y)\\&=2s\psi_0\left[e^{\frac{ikn(\sin\theta_1+\cos\theta_1)(x-y)}{2}}+e^{\frac{ikn(x-y)}{2}+i\varphi}\right].\end{aligned} \tag{4}$$

Here $t=1+r\approx 2$ is the evanescent wave amplitude, n is the refractive index of the prism, and θ_1 is the refraction angle of the single-photon beam within the prism, which satisfies Snell's law as $n\sin\theta_1=\sin\theta$. Mathematically, Eqs. (1)–(4) are the solutions to Schrödinger equation for photon in this WM-MZI instrument. What do they mean? This deserves a careful quantum mechanical analysis and interpretation. From the orthodox quantum physics, it follows that the wave function represents the spatial probability amplitude distribution of quantum objects, including photons. In this framework, the two important physical quantities in Eqs. (1)–(4), r and s, represent the single-photon probability wave reflection and scattering coefficient, whereas $R=|r|^2$ and $S=|s|^2$ denote the reflection and scattering probability of the single photon on the prism surface. Under the condition of small S and large R, we find $S+R\approx 1$. Now from Eqs. (1)–(4), we obtain the single-photon light intensities of the two output paths as

$$P_{1,\mathrm{out}}=|\psi_{1,\mathrm{out}}(x,y)|^2=RP_0, \tag{5a}$$

$$P_{2,\mathrm{out}}=|\psi_{2,\mathrm{out}}(x,y)|^2=RP_0, \tag{5b}$$

where $P_0=|\psi_0|^2$ is the single-photon light intensity at the input. The intensity distribution of the interference reads

$$\begin{aligned}P_{\mathrm{scat}}&=A|\psi_{\mathrm{scat}}(x,y)|^2=8SAP_0\\&\times\left\{1+\cos\left[\frac{(kn\sin\theta_1+kn\cos\theta_1-kn)(x-y)}{2}+\varphi\right]\right\},\end{aligned} \tag{6}$$

where A is the combined collection and detection efficiency and is usually much smaller than 100%. In the above theoretical analysis, we have assumed a 100% transmission of photon through the two right-angle sides of the prism.

The next important step is to calculate the path distinguishability D and the interference pattern fringe visibility V. Let us first make a brief analysis on what happens for a photon coming from beams 1 and 2. If the prism is not coated with a weakly scattering thin film, the total internal reflection is perfect, i.e., $r = 1, R = 1, s = 0$. Thus, the photon will follow its own path and transport unambiguously to photodetectors APD1 and APD2, respectively. In this case the path distinguishability is 100%, while the interference pattern, although existing there at the prism hypotenuse outer surface, cannot be detected and thus the fringe visibility is zero. Yet, with the milk-coated prism surface as the interference screen, i.e., $r < 1, R < 1, s > 0$, and according to Eq. (6), it is possible to detect the interference pattern. Although the overall intensity $8SAP_0$ is low because of the small value of S and A, the fringe visibility V theoretically can be as high as 1. The value of the path distinguishability can be estimated according to a simple model as follows. For each arm of the WM-MZI, i.e., the reflection beam 1 and beam 2, if no scattering-induced deviation of the photon from its original path, the reflectivity should be ideally 100%. Now since scattering does occur, the extent of deviation of each photon from its original path is measured by the actual reflectivity R, and thus the path distinguishability is taken simply as $D \approx R$.

In the following, we discuss the experimental results of the WM-MZI and clearly show that simultaneous observation of the path and interference of single photons is achievable. As shown in the inset of Fig. 4(a), the optical path length of path 2 can be tuned by changing the position of the wedge plate (wedge angle 0.5°) along the direction of the arrow. By tuning the wedge plate and using a fixed slit in front of APD3, we are able to measure the effect of longitudinal interference, i.e., interference with respect to phase shift φ, according to Eq. (6), by simultaneously counting single photons at three channels by using three APDs. The color-code traces in Fig. 4(a) indicate the detected photon counts of the output beam 1 and beam 2 in blue and red, respectively. One observes that the photon count levels of the two beams do not change much in particular as the position of the wedge plate is tuned from 0.2 mm to 0.4 mm. The measured photon count rates of APD1 and APD2 are obtained for the bright state of the QD. Specifically, from the fluorescence time traces of the QD, we set a time bin of 10 ms and select the time period with more than five consecutive bright bins and the corresponding photon counts as the effective data to get the correct photon count rate. Thus the time periods when the QD is in dark states emission have been subtracted and only the bright-state photon count rates are shown in Fig. 4 [33]. The small variations of the count rates of the two channels are due to the possible mechanical stability of the setup and the photostability of the QD within about an hour of measurement. For APD3, the detected photon count level is much lower and each data point is integrated for 50 s. Figure 4(b) displays the detected photon count rate

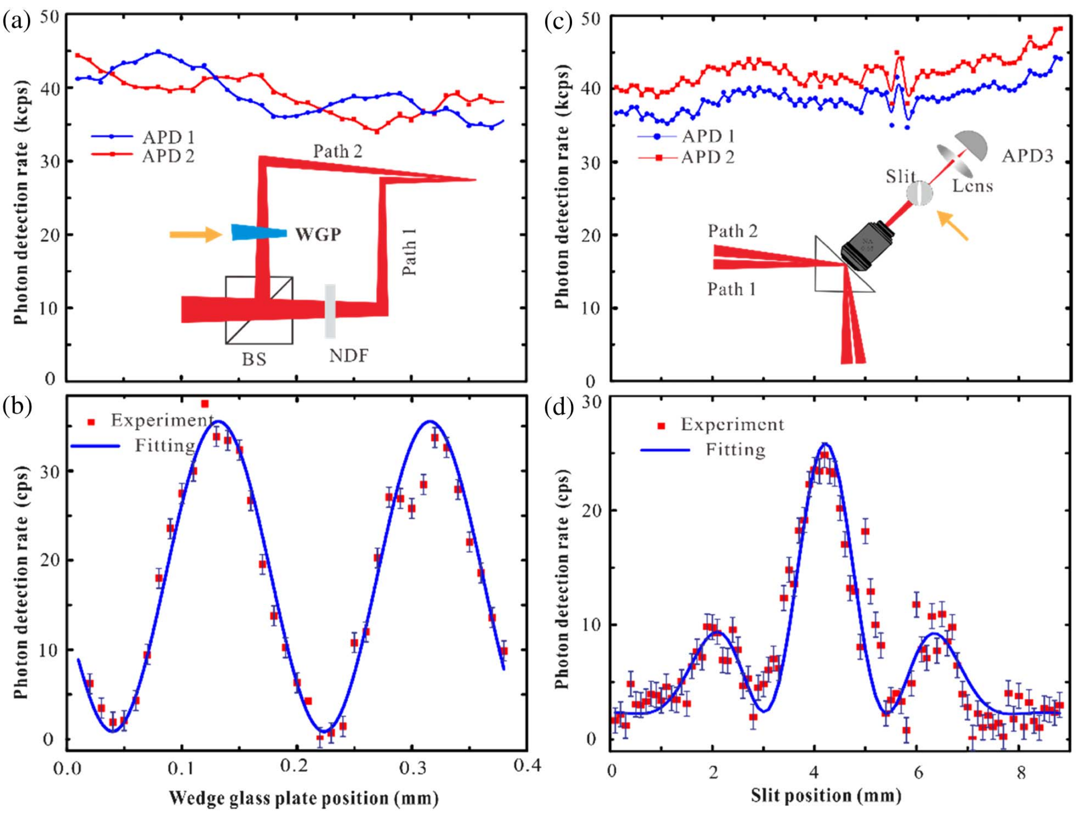

Fig. 4. Simultaneous measurements of path and interference. For longitudinal interference, (a) the photon detection rates of APD1 and APD2 change as a function of the optical path length tuned by the wedge glass plate (WGP); (b) the photon detection rate of APD3. The slit position is fixed in this series of measurements. For transverse interference, (c) the photon detection rates of APD1 and APD2 change as a function of the slit position; (d) the photon detection rates of APD3. The wedge glass plate is fixed in this series of measurements.

of APD3 (dark counts subtracted) as a function of the position of the wedge plate. The position of the APD3 is fixed and the results are insensitive to its position. One observes a very nice periodic change of the signal with respect to the phase shift φ, which is the exciting longitudinal interference effect. The error bar is mainly due to the variation of the dark count rate. The blue trace is a fit to the experimental data points and the visibility of the fringes V is estimated to be 97%.

To directly observe the lateral interference pattern, i.e., the interference with respect to the displacement along the prism hypotenuse outer surface according to Eq. (6), we fix the position of the wedge plate and change the lateral position of the slit and again record the photon count rate in these three channels simultaneously. Note that the slit size is only 150 μm and the interference image extends to about 10 mm. Thus, the slit functions as an imaging sampler along the interference direction. In front of APD3, an aspherical condenser lens with a focal length of 16 mm is used to ensure that the whole spot where the two beams interfere can be imaged onto APD3 if the slit is removed. Therefore, a lateral scan of the slit position gives the image of the interference pattern on the spot. Figure 4(c) displays the detected photon counts of reflected beam 1 and beam 2 in blue and red, respectively. In principle, these channels should not be affected by the change of the slit position, but in practice the signal levels fluctuate due to the fact that during the hour-long measurement the intensity of the QD emission changes gradually because of the drift of the confocal excitation laser spot. The rapid small oscillations are because of the uncertainty in determining the bright state emission rate of the QD. Figure 4(d) shows the measured photon count rate of APD3 as a function of the slit position. One clearly observes the interference feature. On the other hand, the decrease of the fringe contrast with the lateral position difference is due to the finite spot size of the two beams. To evaluate the visibility of the lateral interference pattern, we model the interference with the assumption that two Gaussian beams with the same beam waist partially overlap in space with a small inclination angle. The blue trace in Fig. 4(d) is a fit based on the model to the experimental results. We have estimated the visibility of the interference fringe V to be 0.84 if the two beams were plane waves.

The above experimental data clearly indicates our WM-MZI exhibits an excellent performance for observing the wave property of a single photon manifested from the pronounced interference pattern in both the longitudinal and lateral dimensions. The experiment agrees well with theoretical prediction as made in Eq. (6) and in Ref. [27]. Now we turn our eyes to another entity of wave–particle duality, i.e., the particle property of the photon, which is connected with the path distinguishability D. In experiment, the reflection coefficient R of the milk-coated prism is calibrated by comparing with a silver mirror. As shown in Fig. 3(a), the photon signal is in random status with time elapsing, which means photons randomly emit one by one from a QD, passing through the WM-MZI and detected by the photodetectors. The overall single-photon reflection intensity from the reference silver mirror and the milk-coated prism has a time-averaged quantity of 102 kcps and 81 kcps, respectively.

Considering in practice the reflectivity of the photon from the silver mirror is 95.5%, and the transmission coefficient of the photon through each right-angle side of the prism is 96%, we can calculate the reflection coefficient of photon through the whole prism as $R = 83\%$, and the scattering loss is about 17%. This allows us to estimate the path distinguishability $D \approx R = 83\%$. As a result, we can make a good estimate to evaluate the wave–particle duality. For the longitudinal interference case we obtain $V^2 + D^2 \approx 0.97^2 + 0.83^2 = 1.63 \gg 1$ while for the lateral interference one we have $V^2 + D^2 \approx 0.84^2 + 0.83^2 = 1.39 \gg 1$.

3. DISCUSSION AND CONCLUSIONS

The experimental observations using single photons agree well with the theoretical prediction made strictly in the framework of the standard quantum mechanics formulation for the WM-MZI with a milk-coated prism surface as an interference screen. The weakly scattering interference screen plays a key role in achieving a remarkable interference pattern, which in principle can exhibit a perfect fringe visibility as $V = 1$ and in practice a very high value of $V = 0.97$ is measured, despite that the absolute amplitude of this pattern is several orders of magnitude smaller than the incident single-photon light amplitude. At the same time, the two beams remain sufficiently high path distinguishability D. Thus, this WM-MZI indeed can allow one to observe simultaneously the wave and particle features of the photon with a power much higher than that enabled by the well-established principle of wave–particle duality. In contrast to previous works [14,36] using a quantum beam splitter where the orthodox limit of $V^2 + D^2 \le 1$ always holds when the total photon number is taken into account, our work here clearly goes beyond the limit even in the ensemble sense. We expect a better performance of obtaining $V = 1$, $D \to 1$ is achievable by improving the quality of the single-photon source, the diffusive milk-coating interference screen, the transmissivity through the right-angle side of the prism, the collection and detection efficiencies, and so on.

Our experiment allows one to draw a basic physical picture of the whole journey a photon takes within the WM-MZI. A photon emitted from the QD source goes into the WM-MZI, passes the BS, goes to and transports along either path 1 or path 2, hits and goes into the prism horizontally, hits the hypotenuse surface and is reflected downward vertically, and finally goes into the two photodetectors and triggers a photon counting event. This journey seems to be very ordinary, well known, and understood, and nothing unexpected happens. However, when one looks closely at the hypotenuse surface of the prism, which is now coated with an everyday milk film, using some highly sensitive state-of-the-art single-photon detection and imaging instruments, something miraculous happens. Right at the hypotenuse outer surface, a very clear interference pattern forms as more and more photons go into the WM-MZI when time goes on. A strange thing is that the fringe visibility is as perfect as comparable to the well-known case when an ordinary laser beam is used to perform the same experiments. In the language of quantum physics, the wave nature of the photon is perfectly observed. The price to achieve this beautiful status is that the photon now does not follow strictly its original path of transport; however, the deviation is only a little bit, and it can be managed and reduced to a very low level when better instruments are used, so that one can be very sure (not 100% but close) of the path the photon eventually takes. Or in the language of quantum physics, one can observe very good particle nature of the photon. This is drastically different from the usual delayed-choice MZI scheme as illustrated in Fig. 1(a), where once perfect interference pattern is observed, and the path each photon takes becomes completely ignorant to the observer.

Another thing that is worthwhile to notice and discuss here concerns the origin of the interference pattern formed at the prism hypotenuse outer surface and recorded by the imaging and detecting system via APD3. Some people might argue that this pattern is formed only by the small set of scattered photons that go into the APD3, while the remaining big set of photons detected by APD1 and APD2 measure the path distinguishability information. Thus, it is not justified to conclude violation of the orthodox wave–particle duality. We argue here that according to the theoretical analysis of Eqs. (1)–(6), the small set of photons detected by APD3 are the faithful representation (in terms of interference pattern formation) of the whole incident photons at the entrance of the WM-MZI. The fringe visibility V determined here is thus exactly the right quantity for the interference pattern formed by the whole photons at the prism hypotenuse outer surface (in the form of evanescent wave). In addition, the path distinguishability D determined from the detection data of APD1 and APD2 is also rightly the quantity for the whole incident photons. Because we are talking about the detection of wave–particle duality for the photons emitting from the QD and injected into the WM-MZI, it is fully justified to say that the experimental data of $V^2 + D^2 \approx 0.97^2 + 0.83^2 = 1.63 \gg 1$ and $V^2 + D^2 \approx 0.84^2 + 0.83^2 = 1.39 \gg 1$ do hold for the whole incident photons. Therefore, it is fully justified to claim violation of the orthodox wave–particle duality.

As another issue, we would like to notice that we have done experiments in the single experiment setup of the WM-MZI to test the wave–particle duality. This single experiment setup in principle allows one to observe simultaneously the nearly complete wave ($V \to 1$) and complete particle ($D \to 1$) nature of photons and other quantum objects. In contrast, in previous experiments, one essentially needs two different (and essentially exclusive) experiment setups, i.e., one for observing the complete wave nature and the other for observing the complete particle nature. In our experiment and also in all other experiments based on interferometers to observe wave–particle duality of a specific particle, such as a photon, electron, and atom, one sends the particle one by one through the interferometer, and observes, analyzes, and retrieves the wave nature (via interference pattern) and particle nature (path information) based on the accumulation of many events of a single measurement, or in other words, measurement over an ensemble of particles. Such an experiment is historically called a single experiment rather than many experiments, because all the incident particles are equivalent with each other as long as the experimental conditions are strictly kept the same. In this regard, in our current work we have indeed performed a single experiment in one single experimental setup to observe simultaneously the wave and particle nature of photons.

The designed WM-MZI is much more powerful to observe simultaneous the wave and particle nature of the photon than the delay-choice scheme of MZI. It should be emphasized that all these observations are dictated within the reign of standard quantum mechanics and can be predicted by standard calculations. Nonetheless, the physics underlying the unexpected behavior of the photon is indeed going beyond the well-known principle of wave–particle duality. It seems that our experiment does add some mysteries into the already mysterious system of concept upon orthodox quantum mechanics taught by the Copenhagen doctrine. We believe that these experimental studies in a deeper and broader aspect in the future will open up new insights upon the foundation of quantum physics and offer instructive clues as to explore more fundamental physics for the microscopic world beyond contemporary quantum mechanics.

Funding. National Natural Science Foundation of China (11474114, 11874166, 11974119); Guangdong Province Introduction of Innovative RD Team (2016ZT06C594); Thousand-Young-Talent Program of China.

Acknowledgment. We gratefully acknowledge X. Peng, H. Qin, and X. Hou (all of Zhejiang University, China) for providing the colloidal quantum dot sample and the continuous support.

Disclosures. The authors declare that there are no conflicts of interest related to this paper.

†These authors contributed equally to this work.

REFERENCES

1. N. Bohr, "Discussion with Einstein on epistemological problems in atomic physics," in *Albert Einstein: Philosopher Scientist*, P. A. Schilpp, ed. (Library of Living Philosophers, 1949), pp. 200–241; reprinted in Quantum Theory and Measurement, J. A. Wheeler and W. H. Zurek, eds. (Princeton University, 1983), pp. 9–49.
2. R. L. R. Feynman and M. Sands, *The Feynman Lectures on Physics* (Addison Wesley, 1965), Vol. **III**, Chap. I.
3. W. K. Wootters and W. H. Zurek, "Complementarity in the double-slit experiment: quantum nonseparability and a quantitative statement of Bohr's principle," Phys. Rev. D **19**, 473–484 (1979).
4. M. Schlosshauer, "Decoherence, the measurement problem, and interpretations of quantum mechanics," Rev. Mod. Phys. **76**, 1267–1305 (2004).
5. A. D. Cronin, J. Schmiedmayer, and D. E. Pritchard, "Optics and interferometry with atoms and molecules," Rev. Mod. Phys. **81**, 1051–1129 (2009).
6. J. A. Wheeler, "The "past" and the "delayed-choice" double-slit experiment," in *Mathematical Foundations of Quantum Theory*, E. R. Marlow, ed. (Academic, 1978), pp. 9–48.
7. J. A. Wheeler, *Problems in the Formulations of Physics*, G. T. di Francia, ed. (Academic, 1979).
8. M. O. Scully, B.-G. Englert, and H. Walther, "Quantum optical tests of complementarity," Nature **351**, 111–116 (1991).
9. S. Dürr, T. Nonn, and G. Rempe, "Origin of quantum-mechanical complementarity probed by a 'which-way' experiment in an atom interferometer," Nature **395**, 33–37 (1998).
10. P. Bertet, S. Osnaghi, A. Rauschenbeutel, G. Nogues, A. Auffeves, M. Brune, J. M. Raimond, and S. Haroche, "A complementarity experiment with an interferometer at the quantum-classical boundary," Nature **411**, 166–170 (2001).

11. V. Jacques, E. Wu, F. Grosshans, F. Treussart, P. Grangier, A. Aspect, and J.-F. Roch, "Experimental realization of Wheeler's delayed-choice Gedanken experiment," Science **315**, 966–968 (2007).
12. V. Jacques, E. Wu, F. Grosshans, F. Treussart, P. Grangier, A. Aspect, and J. F. Roch, "Delayed-choice test of quantum complementarity with interfering single photons," Phys. Rev. Lett. **100**, 220402 (2008).
13. R. Ionicioiu and D. R. Terno, "Proposal for a quantum delayed-choice experiment," Phys. Rev. Lett. **107**, 230406 (2011).
14. J.-S. Tang, Y.-L. Li, X.-Y. Xu, G.-Y. Xiang, C.-F. Li, and G.-C. Guo, "Realization of quantum Wheeler's delayed-choice experiment," Nat. Photonics **6**, 600–604 (2012).
15. A. Peruzzo, P. Shadbolt, N. Brunner, S. Popescu, and J. L. O'Brien, "A quantum delayed-choice experiment," Science **338**, 634–637 (2012).
16. F. Kaiser, T. Coudreau, P. Milman, D. B. Ostrowsky, and S. Tanzilli, "Entanglement-enabled delayed-choice experiment," Science **338**, 637–640 (2012).
17. S. S. Afshar, E. Flores, K. F. McDonald, and E. Knoesel, "Paradox in wave-particle duality," Found. Phys. **37**, 295–305 (2007).
18. O. Steuernagel, "Afshar's experiment does not show a violation of complementarity," Found. Phys. **37**, 1370–1385 (2007).
19. V. Jacques, N. D. Lai, A. Dréau, D. Zheng, D. Chauvat, F. Treussart, P. Grangier, and J. F. Roch, "Illustration of quantum complementarity using single photons interfering on a grating," New J. Phys. **10**, 123009 (2008).
20. S. Kocsis, B. Braverman, S. Ravets, M. J. Stevens, R. P. Mirin, L. K. Shalm, and A. M. Steinberg, "Observing the average trajectories of single photons in a two-slit interferometer," Science **332**, 1170–1173 (2011).
21. A. Danan, D. Farfurnik, S. Bar-Ad, and L. Vaidman, "Asking photons where they have been," Phys. Rev. Lett. **111**, 240402 (2013).
22. H. Yan, K. Liao, Z. Deng, J. He, Z.-Y. Xue, Z.-M. Zhang, and S.-L. Zhu, "Experimental observation of simultaneous wave and particle behavior in a narrowband single-photon wave packet," Phys. Rev. A **91**, 042132 (2015).
23. A. S. Rab, E. Polino, Z.-X. Man, N. Ba An, Y.-J. Xia, N. Spagnolo, R. Lo Franco, and F. Sciarrino, "Entanglement of photons in their dual wave-particle nature," Nat. Commun. **8**, 915 (2017).
24. B.-G. Englert, "Fringe visibility and which-way information: an inequality," Phys. Rev. Lett. **77**, 2154–2157 (1996).
25. Z.-Y. Li, "Elementary analysis of interferometers for wave—particle duality test and the prospect of going beyond the complementarity principle," Chin. Phys. B **23**, 110309 (2014).
26. Z.-Y. Li, "Time-modulated Hamiltonian for interpreting delayed-choice experiments via Mach-Zehnder interferometers," Chin. Phys. Lett. **33**, 080302 (2016).
27. Z.-Y. Li, "Weak-measurement Mach-Zehnder interferometer for testing wave-particle duality," EuroPhys. Lett. **117**, 50005 (2017).
28. Z.-Y. Li, "Atom interferometers with weak-measurement path detectors and their quantum mechanical analysis," Chin. Phys. B **28**, 060301 (2019).
29. P. Michler, A. Kiraz, C. Becher, W. V. Schoenfeld, P. M. Petroff, L. Zhang, E. Hu, and A. Imamoglu, "A quantum dot single-photon turnstile device," Science **290**, 2282–2285 (2000).
30. H. Qin, Y. Niu, R. Meng, X. Lin, R. Lai, W. Fang, and X. Peng, "Single-dot spectroscopy of zinc-blende CdSe/CdS core/shell nanocrystals: nonblinking and correlation with ensemble measurements," J. Am. Chem. Soc. **136**, 179–187 (2014).
31. K. G. Lee, X. W. Chen, H. Eghlidi, P. Kukura, R. Lettow, A. Renn, V. Sandoghdar, and S. Götzinger, "A planar dielectric antenna for directional single-photon emission and near-unity collection efficiency," Nat. Photonics **5**, 166–169 (2011).
32. G. Nair, J. Zhao, and M. G. Bawendi, "Biexciton quantum yield of single semiconductor nanocrystals from photon statistics," Nano Lett. **11**, 1136–1140 (2011).
33. W. Xu, X. Hou, Y. Meng, R. Meng, Z. Wang, H. Qin, X. Peng, and X. W. Chen, "Deciphering charging status, absolute quantum efficiency, and absorption cross section of multicarrier states in single colloidal quantum dots," Nano Lett. **17**, 7487–7493 (2017).
34. A. L. Efros and D. J. Nesbitt, "Origin and control of blinking in quantum dots," Nat. Nanotechnol. **11**, 661–671 (2016).
35. H. Qin, R. Meng, N. Wang, and X. Peng, "Photoluminescence intermittency and photo-bleaching of single colloidal quantum dot," Adv. Mater. **29**, 1606923 (2017).
36. J.-S. Tang, Y.-L. Li, C.-F. Li, and G.-C. Guo, "Revisiting Bohr's principle of complementarity with a quantum device," Phys. Rev. A **88**, 014103 (2013).